Experimental study on fracture behavior of pre-notched mortar beams using ESPI technique

H.H. CHEN and R.K.L.SU
Department of Civil Engineering
The University of Hong Kong
Pokfulam Road, Hong Kong
klsu@hkucc.hku.hk http://web.hku.hk/~klsu/

Abstract: - Electronic Speckle Pattern Interferometry (ESPI) technique is of high sensitivity and can provide full-field surface deformation. This paper introduces the application of ESPI technique to measure the surface deformation of pre-notched mortar beams in three-point bending tests. In addition to ESPI, Linear Variable Differential Transformers (LVDTs) and clip gauge extensometer were used to measure the mid-span deflection and Crack Mouth Opening Displacement (CMOD) of the beam respectively. Displacements measured by ESPI are compared with that obtained from LVDTs and clip gauge to verify the accuracy of ESPI. From the displacement field measured by ESPI, one of the nonlinear fracture properties of quasi-brittle materials, Crack Tip Opening Displacement (CTOD) was determined and load-CTOD curve is plotted. Furthermore, crack propagation process and Crack Opening Displacement (COD) profiles at different loading stages are presented. Some fracture parameters of the mortar specimen are quantified.

Key-Words: - fracture behavior, mortar beam, ESPI technique, three-point bending

1 Introduction

The fracture behavior of quasi-brittle materials such as concrete and mortar is characterized by a fracture process zone ahead of the main crack. In the fracture process zone, some mechanisms such as micro-cracking, crack deflection, aggregate bridging, and crack branching, make the fracture behavior of the material become very complicated.

In order to understand the fracture process of mortar, the crack propagation in mortar needs to be monitored. This gives rise to the deformation measurement of the mortar with a crack. LVDTs are the most commonly used instrument for measuring displacements. However, it requires a stable installation reference and can only provide displacement information of limited locations of the specimen. For the measurement of crack propagation which requires measuring local deformation, LVDTs are hard to serve the purpose. In the same circumstance, clip gauge is accurate in the measurement of the relative displacement of a narrow gap within 2-4 mm. Clip gauge is particularly suitable to measure the CMOD of the specimen. For other deformation measurement, clip gauge is not feasible due to its installation difficulty. Some researchers used optical fiber sensor to measure the micro-scale deformation of the materials [1-3]. However, the optical fiber sensor can only be located at a specific position and is not applicable to monitor the crack propagation. ESPI can overcome the aforementioned limitations and enable a non-contact full-field surface deformation measurement. It is an effective tool for the investigation of fracture process zone in mortar.

With its high precision, ESPI has been applied to measure the deformation of many materials. Celdolin et al. [4] conducted interferometric measurement on concrete specimens and obtained local stress-strain and stress-separation relations near a notch. Jia and Shah [5] used a two-dimensional ESPI system to monitor the fracture process of concrete. Ezio Cadoni et al. [6] used ESPI to observe the crack propagation of clay specimens. Kim et al. [7] applied ESPI and shearography to measure the deformation of an internal crack of pressure pipeline. Haggerty et al. [8] employed ESPI to observe the fracture deformation of rock. Although, previous studies have shown that ESPI technique is able to measure surface deformations of different materials, quantitative analysis on fracture properties of mortar is limited.

In this study, ESPI technique was used to measure the surface deformation of mortar beams in three-point bending tests. In addition to ESPI, LVDTs and clip gauge were used to measure the mid-span deflection and CMOD of the beam respectively. Displacements measured by ESPI are compared with that obtained from LVDTs and clip gauge to verify the accuracy of ESPI. Fracture parameter CTOD was determined from ESPI results

and load-CTOD curve is plotted. Furthermore, crack propagation process and COD profiles at different loading stages are presented. Some fracture parameters are quantified

2 Principle of ESPI System

The principle of ESPI is based on the interference of two coherent laser beams: reference beam and observation beam. For in-plane measurement, the two beams are reflected and scattered by the rough measuring surface; for out-of-plane measurement, only observation beam is reflected by the surface while the reference beam goes to the sensor directly. The two beams are overlaid and produce a speckle pattern, which is recorded by a Charge Coupled Device (CCD) camera. Fig. 1 shows a schematic setup for the in-plane deformation measurement by ESPI.

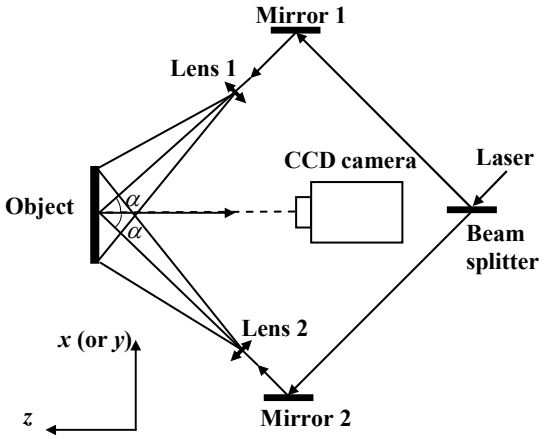

Fig. 1: Schematic of ESPI setup

The intensity, I_m, of the speckle interference pattern is

$$I_m = I_A + I_B + 2\sqrt{I_A I_B}\cos(\phi + \varphi_m) \quad (1)$$

where I_A and I_B are the intensities of the two cohesive beams, ϕ is the interference phase of the two cohesive beams, and φ_m is the introduced phase-shift.

By subtracting two speckle patterns at different states, before and after deformation, interference fringes can be obtained. Using the four-step phase shifting method [9], the interference phase at each state can be determined by four intensities with phases separated by π/2. Assuming the interference phases before and after the deformation are ϕ and ϕ' respectively, the phase difference Δ, also known as wrapping phase map, can be obtained by ϕ'-ϕ.

Applying the phase-shift process, the unwrapping phase map including the displacement field can be obtained. ISTRA software [10] was used to generate displacement contour map.

The in-plane displacement u (or v) can be calculated by

$$u = \frac{\Delta \cdot \lambda}{4\pi \sin\alpha} \quad (2)$$

where α is the incidence angle of the illumination beams, λ is the wavelength of the applied laser, and Δ is the phase difference between the two states: before deformation and after deformation.

Similarly, the out-of-plane displacement w can be obtained by

$$w = \frac{\Delta \cdot \lambda}{2\pi(1+\cos\alpha)} \quad (3)$$

ESPI and can provide non-contact, high-precision, full-field deformation information of different materials. It is particularly useful to measure the surface deformation with high-gradients, such as near a crack tip.

ESPI is so sensitive that it can be easily influenced by external factors such as noise, vibrations and rigid-body motions of the specimen. In order to eliminate the influence of noise and vibrations, tests should be carried out in a relatively quiet circumstance and ESPI sensor should be set on a stable fixture. Measures, such as gypsum packing at the loading points, should be used to reduce the effect of rigid-body motions of the specimen.

Furthermore, ESPI has its inherent limitation that it's only accurate for paraxial region due to the variation of sensitivity vectors. The errors caused by sensitivity vector variation are observable when the measuring zone is not small and the specimen has rigid-body motions. The strain errors caused by rigid-body motions were evaluated by Chen and Su [11]. After the errors being quantified, corrections can be made to eliminate the errors caused by rigid-body motions.

3 Specimen and Experimental Setup

3.1 Specimens and Material Proportions

Pre-notched mortar beams were cast for three-point bending tests. Portland cement was used, and the water/cement ratio was 0.72. Only fine aggregates were mixed in and the maximum aggregate size is 5 mm. Fine aggregate type is medium sand. The concrete mix proportions are tabulated in Table 1. The specimen size (span × depth × thickness) is 400×100×40 mm. The initial notch depth and width

ISBN: 978-960-474-275-2

of the notched beam are 30 mm and 2 mm respectively.

In addition to four beams, two cubes (150×150 ×150 mm) and two cylinders (150×300 mm) were created. After the mortar was cast and cured, the specimens were placed in air (Temperature: 20±2℃; RH: 75-85%) until the date of testing. The cubes were tested to determine the cube compressive strength f_{cu}, and the cylinders were tested to obtain the elastic modulus E. After 28 days, specimens were tested. The compressive strength f_{cu} and elastic modulus E are 25.6 MPa and 19016 MPa respectively.

Table 1: Material proportions by weight

Material	kg/m^3
Water	240
Cement	333
Fine Aggregate	1735

3.2 Experimental Setup

Using an MTS bending fixture, three-point bending tests on the mortar beams were carried out. The experimental setup is presented in Fig. 2(a). In the test, displacement control with a loading rate of 0.01 mm/min of the jack displacement was adopted. Clip gauge with a resolution of 1 μm was installed to measure the CMOD of the beam, as shown in Fig. 2(a). LVDTs with a resolution of 2 μm were employed to measure the mid-span deflection. In order to measure the mid-span deflection without support disturbances, an additional frame was located on the top of the beam to act as a reference datum of LVDTs. The LVDTs were located vertically to measure the deflection of the beam, as shown in Fig. 2(b). The load-deflection and load-CMOD curve of the entire process were recorded by a data logger.

(a)

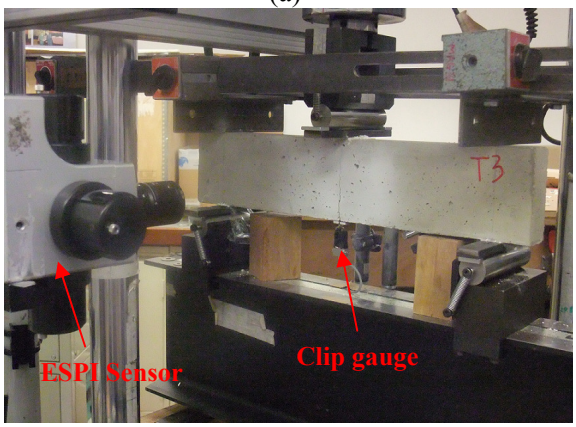

(b)

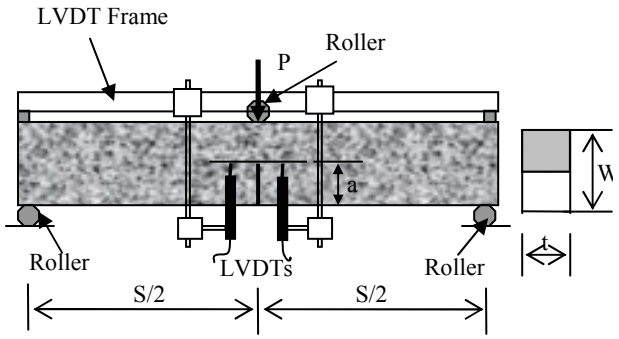

Fig. 2 (a): Experimental setup; (b) Arrangement of LVDTs

A three-dimensional ESPI system (Q300 produced by Dantec-Ettemeyer) was used to measure the surface deformation. The specifications of Q300 system are tabulated in Table 2. In the test, deformation map of the measuring surface was captured by a CCD camera in a step-by-step manner until the beam failed. To reduce the influence of any possible ambient vibrations, the camera was set on a fixture frame which moved with the jack.

Table 2: Technical specifications of Q300 system

Displacement accuracy	0.03 - 1 μm adjustable
CCD-resolution	1380 × 1035 pixels
Measuring range	Adjustable, 10 - 100 μm per step depending on measuring direction
Measuring area	Up to 200 × 300 mm² with built in illumination, larger areas with external laser
Working distance	Variable, 0.2...1.0 m
Laser (built in)	Diode, 2 × 75 mW, λ=785 nm
Data processing	Dantec Dynamics software ISTRA

4 Experimental Results

In a pre-notched beam, the main crack initiated from the tip of the notch and propagated to the upper support. Due to the existence of the aggregates, the crack path could not keep a straight line and changed direction in order to round the obstacle, presenting sinuosity in its trajectory.

4.1 Load-CMOD Curve

ISBN: 978-960-474-275-2

In ESPI results, CMOD can be obtained from the displacement field in the x-direction. Fig. 3(a) shows the displacement contour in the x-direction.

When the beam is bent, below the neutral-axis, the part on the left of the notch deforms leftward and the part on the right deforms rightward, thus the lower part is in tension. CMOD can be determined from the relative displacement of left and right face of the notch, as shown in Fig. 3(a).

$$CMOD = u_{right} - u_{left} \quad (4)$$

where u_{right} is the displacement of the right face at crack mouth; u_{left} is the displacement of the left face at crack mouth.

A comparison of load-CMOD curves is presented in Fig. 3(b). From the figure, it can be found that ESPI results are in good agreement with the CMOD measured by clip gauge. At peak load, the corresponding CMOD is about 35-40 μm.

(a)

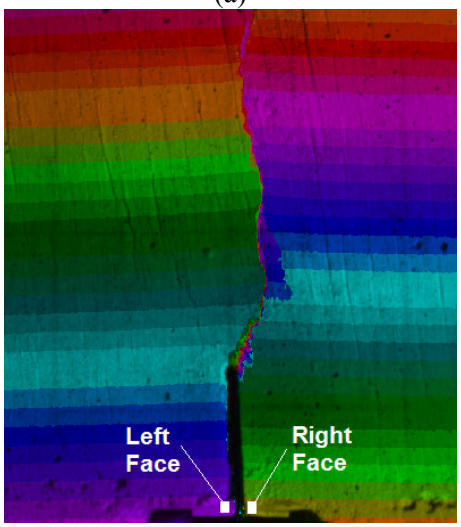

(b)

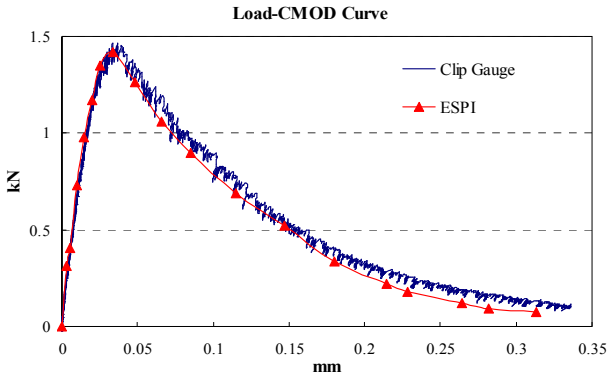

Fig. 3: (a) Displacement contour in the x-direction; (b) Comparison of load-CMOD curves

4.2 Load-deflection Curve

In ESPI results, the mid-span deflection of the beam can be obtained from the displacement field in the y-direction. Fig. 4(a) describes the displacement contour in the y-direction.

(a)

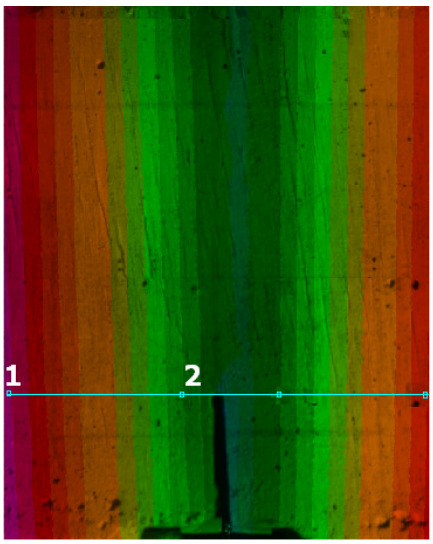

(b)

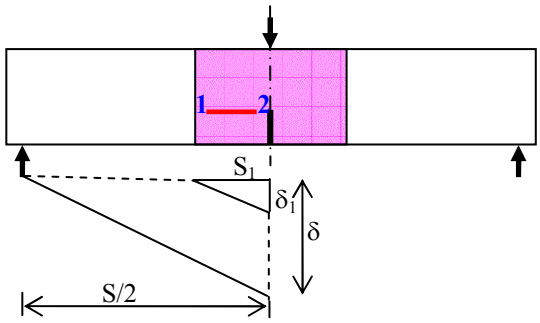

(c)

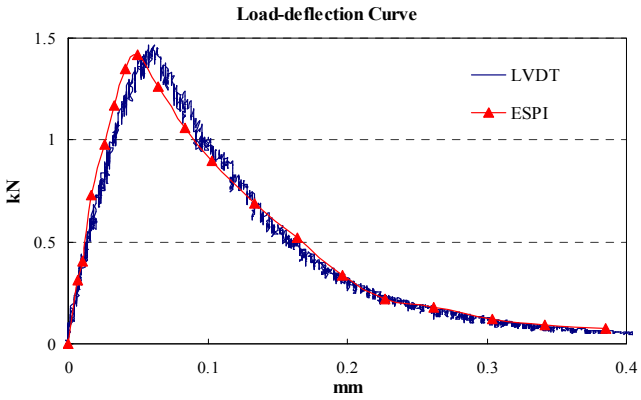

Fig. 4: (a) Displacement contour in the y-direction; (b) Schematic illustration of mid-span deflection; (c) Comparison of load-deflection curves

When the beam is bent, the part near the mid-span moves downward while the part near the end of the beam moves upward. The mid-span deflection of the

ISBN: 978-960-474-275-2

beam can be determined from the relative displacement of the end and the mid-span.

Since the measuring zone is only concentrated near the mid-span of the beam, the deflection in the middle part of the beam δ_1 can be obtained directly from the displacement field in the y-direction.

$$\delta_1 = v_1 - v_2 \tag{5}$$

where v_1 and v_2 are the displacements of points 1 and 2 respectively, as described in Fig. 4 (a) and (b).

The deflection of the whole beam δ is determined according to linear interpolation, as shown in Fig. 4(b). The deflection of the beam δ can be estimated proportionally by

$$\delta = \frac{S/2}{S_1} \cdot \delta_1 \tag{6}$$

where S=400mm is the span of the beam; S_1 is the horizontal distance between point 1 and 2.

A comparison of load-deflection curve is shown in Fig. 4(c). ESPI results are in good agreement with the deflection measured by LVDTs. At peak load, the corresponding deflection is about 50-60 μm.

By comparing the ESPI results and LVDTs/clip gauge readings, the accuracy of ESPI is verified. Using the ESPI results, the CTOD was determined in a similar way with CMOD. Load-CTOD curve is shown in Fig. 5. From the figure, it can be found that, at the peak load, the CTOD is about 18 μm. CTOD is significant in the Two-Parameter Fracture Model proposed by Jenq and Shah [12]. According to the model, the crack extension or fracture may be assumed to occur when the CTOD exceeds a critical value.

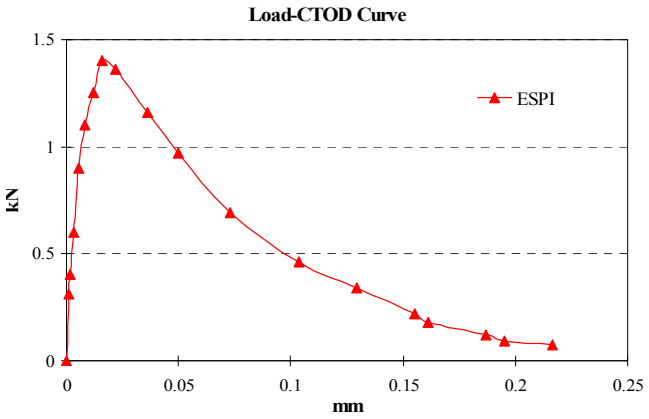

Fig. 5: Load-CTOD curve measured by ESPI

4.3 Crack Propagation Process

Using the ESPI, a crack is recognized as a discontinuity of fringe patterns and displacement contours. Crack propagation process was monitored and recorded by the ESPI sensor.

4.3.1 Fringe Patterns at Different Loading Steps

From the fringe patterns shown in Fig. 6, it is possible to grasp the evolution of the crack. At the early stage of the loading process, the applied load was low (F=0.73kN). The crack did not initiate, as shown in Fig. 6(a). As the loading displacement increased, the crack initiated and developed slowly, as shown in Fig. 6(b). When crack propagated to a certain depth (Fig. 6(c)), which was about half of the beam depth, the crack propagated up quickly and load reached to its peak. After that the load dropped and the crack propagated quickly, as shown in Fig. 6(d). After the load dropped to a certain stage, the crack propagated slowly, as shown in Fig. 6(e).

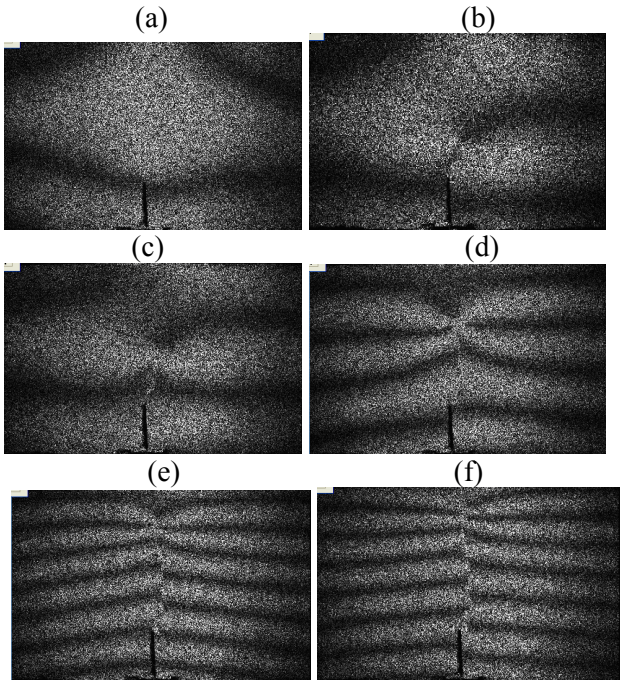

Fig. 6: Fringe patterns at different loading stages: (a) F=0.73 kN; (b) F=1.35 kN; (c) F=1.42 kN; (d) F=1.06 kN; (e) F=0.69 kN; (f) F=0.46 kN

4.3.2 COD Profiles along Crack Faces

COD profiles at different loading stages are presented in Fig. 7.

ISBN: 978-960-474-275-2

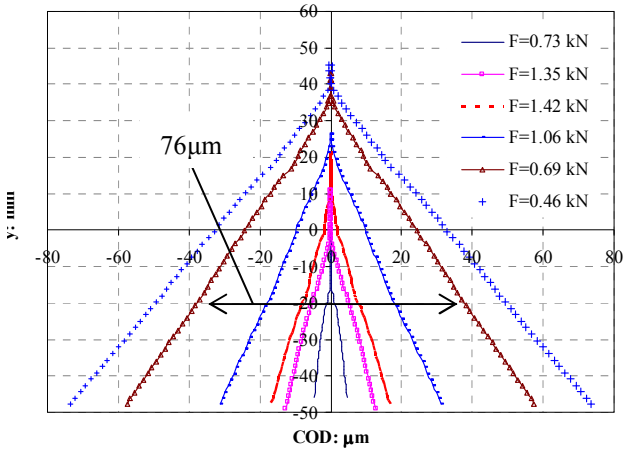

Fig. 7: COD profiles at different loading stages

The minimum separation of crack faces that can be differentiated by ESPI was about 2 μm. After the loading step 11 (F=0.69 kN), the crack depth did not propagate obviously while the load dropped and COD increased much. This is due to the opening of the crack near the notch tip. Once the crack opens, it can't sustain any stress. In Fig. 7, when F=0.69 kN, the COD of the notch tip (y=-20 mm) is approximately 76 μm. This value can provide some reference for the estimation of the minimum crack width for an open crack in mortar.

5 Conclusion

ESPI was used to measure the surface deformation of pre-notched mortar beams in three-point bending tests. The following conclusions can be obtained:

(1) By comparing the displacements measured by ESPI and LVDTs/clip gauge, the accuracy of ESPI is verified. This study demonstrates the feasibility of ESPI technique to measure surface deformation.

(2) It is possible to obtain load-CTOD curves by using ESPI. CTOD is an important parameter to estimate the nonlinear fracture property of quasi-brittle materials according to the Two-Parameter Fracture model.

(3) From the fringe patterns, the crack propagation process was recorded. This information is useful to understand the failure process of the mortar beams.

(4) From the COD profiles at different loading stages, it is possible to quantitatively analyze the fracture process of mortar specimens. Experimental results show that the minimum width of a crack that can be observed by ESPI sensor is about 2 μm. The minimum width for an open crack is about 80 μm. These two widths are useful in the analysis of tensile softening law of mortar.

References:

[1] Q. Li, G. Li, G. Wang and L. Yuan, CTOD Measurement for Cracks in Concrete by Fiber Optic Sensors, *Optics and Lasers in Engineering*, Vol. 42, No. 4, 2004, pp. 377-388.

[2] I. Lee, Y. Libo, F. Ansari and H. Ding, Fiber-optic Crack-tip Opening Displacement Sensor for Concrete, *Cement and Concrete Composites*, Vol. 19, No. 1, 1997, pp. 59-68.

[3] Z. Zhang and F. Ansari, Embedded Crack Tip Opening Displacement Sensor for Concrete, *Sensing Issues in Civil Structural Health Monitoring*, Chapter VII, 2005, pp. 453-462.

[4] L. Cedolin, S.D. Poli and I. Iori, Tensile Behavior of Concrete. *Journal of Engineering Mechanics-Asce*. Vol. 113, 1987, pp. 431-449.

[5] Z.L. Jia and S.P. Shah, Crack Detection in Concrete Using Real-time ESPI Technology. *Nondestructive Evaluation of Aging Aircraft, Airports, Aerospace Hardware, and Materials.* Vol. 2455, 1995, pp. 385-391.

[6] E. Cadoni, B. Bowe and D. Albrecht, Application of ESPI Technique to Evaluate the Crack Propagation Zone of Pre-notched Clay Elements, *SPIE,* Vol. 3407, 1998, pp 410-415.

[7] K.S. Kim, K.S. Kang, Y.J. Kang and S.K. Cheong, Analysis of an Internal Crack of Pressure Pipeline using ESPI and Shearography, *Optics and Laser Technology,* Vol. 35, 2003, pp. 639-643.

[8] M. Haggerty, Q. Lin and J.F. Labuz, Observing Deformation and Fracture of Rock with Speckle Patterns, *Rock Mechanics and Rock Engineering*, Vol. 43, 2010, pp. 417-426.

[9] J.M. Huntley and H. Saldner, Temporal Phase-Unwrapping Algorithm for Automated Interferogram Analysis. *Applied Optics,* Vol. 32, 1993, pp. 3047-3052.

[10] Dantec-Ettemeyer, *ISTRA for Windows, Version 3.3.12.* Dantec Ettemeyer GmbH, Ulm, Germany, 2001.

[11] H.H. Chen and R.K.L. Su, Study on Fracture Behaviors of Concrete Using Electronic Speckle Pattern Interferometry and Finite Element Method, *ICCES*, Vol. 15, No. 3, 2010, pp.91-101.

[12] Y. S. Jenq and S. P. Shah, Two Parameter Fracture Model for Concrete, *Journal of Engineering Mechanics*, Vol. 111, No. 10, 1985, pp. 1227-1241.